EURASIP Journal on Wireless Communications and Networking 2004:1, 74–83

Rotated Walsh-Hadamard Spreading with Robust Channel Estimation for a Coded MC-CDMA System

Ronald Raulefs
Research Group for Mobile Radio Transmission, Institute of Communications and Navigation, German Aerospace Center (DLR), Oberpfaffenhofen, 82234 Wessling, Germany
Email: ronald.raulefs@dlr.de

Armin Dammann
Research Group for Mobile Radio Transmission, Institute of Communications and Navigation, German Aerospace Center (DLR), Oberpfaffenhofen, 82234 Wessling, Germany
Email: armin.dammann@dlr.de

Stephan Sand
Research Group for Mobile Radio Transmission, Institute of Communications and Navigation, German Aerospace Center (DLR), Oberpfaffenhofen, 82234 Wessling, Germany
Email: stephan.sand@dlr.de

Stefan Kaiser
Research Group for Mobile Radio Transmission, Institute of Communications and Navigation, German Aerospace Center (DLR), Oberpfaffenhofen, 82234 Wessling, Germany
Email: stefan.kaiser@dlr.de

Gunther Auer
NTT DoCoMo Euro-Labs, 80687 Munich, Germany
Email: auer@docomolab-euro.com

Received 1 November 2003; Revised 2 April 2004

We investigate rotated Walsh-Hadamard spreading matrices for a broadband MC-CDMA system with robust channel estimation in the synchronous downlink. The similarities between rotated spreading and signal space diversity are outlined. In a multiuser MC-CDMA system, possible performance improvements are based on the chosen detector, the channel code, and its Hamming distance. By applying rotated spreading in comparison to a standard Walsh-Hadamard spreading code, a higher throughput can be achieved. As combining the channel code and the spreading code forms a concatenated code, the overall minimum Hamming distance of the concatenated code increases. This asymptotically results in an improvement of the bit error rate for high signal-to-noise ratio. Higher convolutional channel code rates are mostly generated by puncturing good low-rate channel codes. The overall Hamming distance decreases significantly for the punctured channel codes. Higher channel code rates are favorable for MC-CDMA, as MC-CDMA utilizes diversity more efficiently compared to pure OFDMA. The application of rotated spreading in an MC-CDMA system allows exploiting diversity even further. We demonstrate that the rotated spreading gain is still present for a robust pilot-aided channel estimator. In a well-designed system, rotated spreading extends the performance by using a maximum likelihood detector with robust channel estimation at the receiver by about 1 dB.

Keywords and phrases: code division multiaccess, Walsh-Hadamard spreading sequences, multicarrier, fading channels, concatenated channel coding.

1. INTRODUCTION

Multicarrier code-division-multiple access (MC-CDMA) is a promising candidate for the downlink for the fourth generation of mobile radio systems. MC-CDMA systems offer the spectral efficiency of orthogonal frequency division multiplexing (OFDM) combined with CDMA to combat multiuser interference losses and to offer a flexible multiuser access scheme. However, in a fully loaded system, MC-CDMA experiences a significant loss of performance

due to multiple-access interference. Mobile system operators, for example, in Germany, have paid tremendous amounts of money for licenses of the third mobile radio generation. Therefore, it is essential to identify solutions for fully loaded systems with high spectral efficiency in the presence of multiple-access interference. One solution is to perform complex interference cancellation. These schemes are proposed to enhance the system performance of multiuser systems [1, 2]. The complexity of multiuser detectors (MUDs) depends on the maximum number of users to detect. In addition, a cellular system offers more flexibility with shorter spreading codes. As the cells of a mobile radio system reduce further to increase data rates, especially in hotspots, intercellular interference is more likely. Combining the users in several small user groups allow by explicit use of frequency bandwidths for a distinct user group at the radio cell boundaries to avoid intercellular interference. The spectral efficiency in a cell would be reduced, but the system would be flexible as long as the number of users in a user group is small. On the other hand, performance gains through exploitation of diversity by the spreading code increase with the length of the spreading code. A reasonable spreading length is based on the overall system parameters.

1.1. Signal space diversity

In this paper, we focus on an MC-CDMA system with a high-rate convolutional channel code and rotated spreading sequences. Both combined allow to exploit diversity in Rayleigh faded channels more efficiently. Rotated spreading sequences are derived from signal space or modulation diversity approaches. In the following, we briefly recap some references that focus on signal space diversity.

Signal space or modulation diversity defines a multidimensional signal constellation. The signal constellation is transmitted over different, ideally independently faded channels. The latter could be realized, for example, by interleaving. A high spectral efficiency without the reduction through redundancy, for example, through channel coding, could be accomplished by these diversity schemes. Boullé and Belfiore [3] presented an N-dimensional modulation scheme to exploit time diversity with a lattice decoder. Kerpez presented a coordinated modulation diversity scheme for several channels of a digital subscriber line [4]. The performance improves significantly for Rayleigh faded channels by taking into account a small performance loss for the AWGN channel. DaSilva and Sousa [5] introduced a fading-resistant modulation scheme by transmitting the distinct signal points on different, uncorrelated transmitter antennas. Boutros and Viterbo [6] presented a rotated approach of the modulation alphabet that comes close to the AWGN channel bound for a Rayleigh fading channel. It does not perform worse without rotated modulation in case of an AWGN channel. Latter is identified as an important fact that no degradation occurs in AWGN channels.

In [7], Lamy and Boutros compared Walsh-Hadamard sequences and rotated lattice structures (random and algebraic rotations). They investigated the different schemes for a 16-QAM modulation alphabet. The authors could show that the possible diversity gains for rotated lattices in a Rayleigh fading channel are especially significant in comparison to short lengths of the Walsh-Hadamard sequences. They further demonstrated that for a dimension of 512, the diversity gains for the rotated lattice structures and the pure Walsh-Hadamard approach differ only marginally. In [8], Brunel applied a lattice decoder for an MC-CDMA system. The author construes the possible dimensions generated by the Walsh-Hadamard sequences as an N-dimensional sphere. He used this approach to detect and decode the generated chips by a lattice decoder. In [9], Bury et al. picked up the idea of rotating the data symbols, and applied that to a CDMA system. The authors investigated rotated spreading for BPSK in an uncoded MC-CDMA system.

All of these schemes have in common omitting any redundancy through channel coding. However, channel coding is in multicarrier systems a vital source to improve the performance significantly [10]. In [11], the authors investigated a turbo-coded OFDM system applying modulation diversity. Channel coding and a direct-sequence CDMA system have been investigated in [12] as a concatenated channel code. They construe the spreading code as a block code. The block code combined with the convolutional channel code is a concatenated system that improves its performance as the overall Hamming distance increases through the concatenation and with it the slope of the bit error rate (BER) performance versus the signal-to-noise ratio (E_b/N_0).

1.2. System aspects

The performance of OFDMA compared to MC-CDMA for a fully loaded system depends on the channel coding rate and the ability of the channel code to exploit diversity. For higher channel codes, for example, a channel coding rate $R > 2/3$, OFDMA performs worse than MC-CDMA in a perfectly interleaved scenario even with a single-user detector (SUD), like the MMSE detector [2]. A similar scheme like MC-CDMA is code-division multiple OFDMA (CDM-OFDMA) [2], where the data symbols of one user are spread and transmitted combined in a spreading block. The use of the same data symbols within one spreading block allows applying this scheme with similar performance also in the uplink (neglecting any cellular effects). However, in the uplink, the CDM-OFDM scheme is not affected by interfering data from different users with differently faded channels like it would be in the uplink for MC-CDMA.

Multicarrier systems based on OFDM have shown that they perform poorly without any channel coding [10] in time- or frequency-selective Rayleigh fading channels. Combining spectral efficiency with channel coding calls for high-rate channel codes, which can be realized by rate-compatible punctured convolutional codes (RCPC codes) [13]. RCPCP codes are derived by puncturing good channel codes (mother code). The main advantage of RCPC codes is that the decoder is the same as for the mother code of the RCPC code. However, the Hamming distance is decreased significantly through the higher channel code rate. This makes it harder

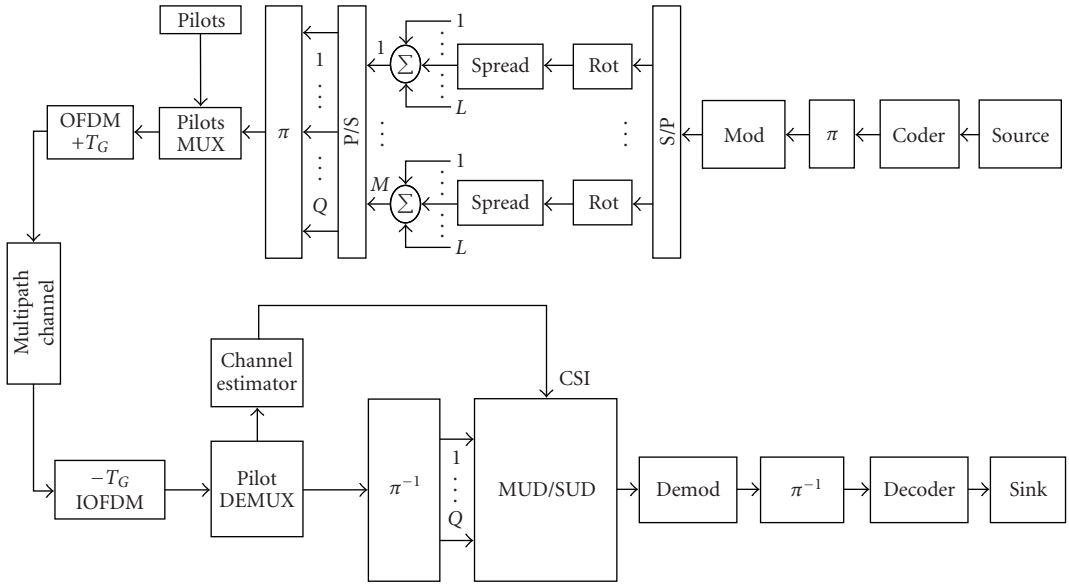

Figure 1: The MC-CDMA system with rotated spreading applied at the transmitter.

to collect the possible diversity in a selectively Rayleigh faded wireless system.

1.3. Rotated spreading

In this paper, we would like to follow the idea of Bury et al. [9]. The authors showed in their publication that rotated spreading applied to uncoded systems with BPSK as the chosen modulation alphabet improves the performance significantly. In [14], it was shown that the performance of uncoded systems for 4-QAM is improved by 3 dB at a BER of 10^{-3} with a maximum likelihood sequence estimation (MLSE) detector and does not improve for a minimum mean square error (MMSE) detector. In addition, it was shown that significant improvements are possible in coded systems for high channel code rates of $R = 5/6$, if they apply a maximum likelihood symbol-by-symbol estimator (MLSSE) detector. In this paper, we add results for $R = 3/4$ and show that the performance depends on the Hamming distance and the constraint length of the chosen convolutional code. We investigate how the performance of rotated spreading is affected by robust channel estimation versus perfect knowledge of the channel fading coefficient on each subcarrier. Diversity is increased by a higher time variability caused by a higher Doppler spread. This increases the MMSE of the channel estimate, but as we will see, even for nonperfect channel state information, the diversity is still exploited.

The paper is organized as follows. In Section 2, we present the used system model with the multipath channel, the channel estimator, and the detectors in detail. Section 3 explains the basis of the possible improvements for an MC-CDMA system. Simulation results in Section 4 show the improvements for different channels, Hamming distances, perfect channel estimation, and two one-dimensional (1D) Wiener filtering. Finally, in Section 5, we conclude and give a brief outlook.

Table 1: Main system parameters.

Parameter	Characteristic/value
Bandwidth	101.5 MHz
Subcarriers	768
Subcarrier spacing	131.836 kHz
Doppler spread	1% (0.01%)
OFDM symbols/frame	48
Users	4 (full load)
User groups	3
Data symbols/OFDM symbol	64
Spreading factor	4
Data modulation	4-QAM
Code bit interleaver (π)	Random interleaver
Subcarrier interleaver (π)	1D random interleaver
Channel coding rate (punctured)	2/3, 3/4, 3/4, 3/4
Generator polynoms octal	(5, 7), (5, 7), (15, 17), (133, 171)
Hamming distance (d_H)	3, 3, 4, 5
Channel estimation	2×1-dimensional Wiener filtering

2. SYSTEM MODEL

In this section, the system model is presented. Figure 1 represents the block diagram of a synchronous MC-CDMA system in the downlink. Table 1 depicts the main system parameters. At the transmitter side, there is a binary source for each of

the K users. The bits of each user are encoded by a convolutional encoder. The code bits are interleaved by a random code bit interleaver to have more independently distributed errors at the receiver. The symbol mapper assigns the bits to complex-valued data symbols according to different alphabets, like PSK or QAM with the chosen cardinality. A serial-to-parallel (S/P) converter allocates the modulated signals to M data symbols per user. Each of the M data symbols is rotated and spread with a Walsh-Hadamard sequence of the length L ($K \leq L$) and multiplexed. The combination of rotating and multiplying each data symbol with a specific Walsh-Hadamard sequence is defined as rotated spreading. It is like column rotation of the original Walsh-Hadamard spreading matrix by specific angles:

$$\begin{aligned} \mathbf{W}_{\text{rot}} &= \mathbf{W}_{\text{org}} \cdot \text{diag}(\mathbf{u}), \\ \mathbf{u} &= \left[u_1, u_2, \ldots, u_K\right]^T,\ u_i = e^{j(2\pi/B)\cdot(k/K)},\ k = 1, \ldots, K, \end{aligned} \tag{1}$$

where $\mathbf{W}_{\text{org}}$ is the Walsh-Hadamard matrix that is used for spreading the different user signals of a user group and $\mathbf{W}_{\text{rot}}$ is the rotated transform of $\mathbf{W}_{\text{org}}$; diag($\mathbf{u}$) defines a diagonal matrix with the elements $\mathbf{u}$ on the diagonal. k represents the k'th user $1, \ldots, K$; B is a constant that is defined by the modulation cardinality for the PSK alphabet. It is 4 for 4-QAM, and 8 for the 16-QAM alphabet. The QAM alphabet is constructed by several differently weighted PSK modulated rings. The maximum points on any of those rings define the constant B. This derives the step size of the rotation angle that is $2\pi/B$. All modulated and spread signals are combined and form one user group. There are Q user groups and each user group has $M \cdot L$ data chips which are interleaved by a random subcarrier interleaver. The interleaved chips are OFDM modulated and cyclically extended by the guard interval. The resulting OFDM signal is transmitted over a multipath channel and corrupted by white Gaussian noise. The different multipath channel models are described in Section 2.4. The receiver converts the received signal in the baseband and removes the guard interval. The remaining symbols are OFDM demodulated and deinterleaved. The pilot demultiplexer removes the pilots and feeds them into the channel estimator. The 2×1-dimensional Wiener filtering channel estimator is explained in Section 2.1. A demultiplexer identifies the user group of interest out of the Q different user groups and detects the signal of the desired user with SUD or MUD. The SUD is performed by the MMSE detector, and the MUD by the MLSSE for a coded MC-CDMA system. Subsequently, the equalized signal is despread. Then all data symbols of the desired user are combined to a serial data stream. The symbol demapper maps the data symbols into bits and calculates the log-likelihood ratio (LLR) for each bit based on the selected alphabet. The code bits are deinterleaved and finally decoded using soft-decision algorithms.

2.1. Pilot-symbol-aided channel estimation with a robust Wiener filter

The received symbols of an OFDM frame are given by

$$R_{n,l} = H_{n,l}S_{n,l} + Z_{n,l}, \quad n = 1, \ldots, N_c,\ l = 1, \ldots, N_s, \tag{2}$$

where $S_{n,l}$, $Z_{n,l}$, N_c, and N_s are the transmitted symbols, the AWGN component, the number of subcarriers per OFDM symbol, and the number of OFDM symbols per frame. The set of pilot positions in an OFDM frame is $\mathcal{P}$ and the number of pilot symbols is $N_{\text{grid}} = \|\mathcal{P}\|$.

The first step in the channel estimation stage is to obtain an initial estimate $\check{H}_{n',l'}$ of the channel transfer function (CTF), that is,

$$\check{H}_{n',l'} = \frac{R_{n',l'}}{S_{n',l'}} = H_{n',l'} + \frac{Z_{n',l'}}{S_{n',l'}}, \quad \forall \{n', l'\} \subset \mathcal{P}. \tag{3}$$

In a second step, the final estimates of the complete CTF are obtained from the initial estimates $\check{H}_{n',l'}$ by two-dimensional (2D) filtering:

$$\hat{H}_{n,l} = \sum_{\{n',l'\} \in \mathcal{T}_{n,l}} \omega_{n',l',n,l} \check{H}_{n',l'}, \tag{4}$$

where $\omega_{n',l',n,l}$ is the shift-variant 2D FIR impulse response of the filter, $n = 1, \ldots, N_c$, and $l = 1, \ldots, N_s$ [15]. The subset $\mathcal{T}_{n,l} \subset \mathcal{P}$ is the set of initial estimates $\check{H}_{n',l'}$ that are actually used to estimate $\hat{H}_{n,l}$. The FIR filter coefficients are based on the Wiener design criterion. The optimal Wiener filter has N_{grid} filter coefficients, in which case the subset $\mathcal{T}_{n,l}$ is identical to the set $\mathcal{P}$. The filter coefficients depend on the discrete time-frequency correlation function (CF) of the CTF $\theta_{n-n'',l-l''} = \text{E}\{H_{n,l}H^*_{n'',l''}\}$, for all $\{n'', l''\} \in \mathcal{T}_{n,l}$, and the noise variance σ^2.

Due to the wide-sense stationary uncorrelated scatterers (WSSUS) assumption of the channel, the CF $\theta_{n-n'',l-l''}$ can be separated into two independent parts:

$$\theta_{n-n'',l-l''} = \theta_{n-n''} \cdot \theta_{l-l''}, \tag{5}$$

with $\theta_{n-n''}$ and $\theta_{l-l''}$ representing the discrete frequency and time CF. This allows to replace the 2D filter by two cascaded 1D filters, one for filtering in frequency direction and the second one for filtering in time direction.

The estimates given by the first 1D filter with coefficients $\omega^{[1]}_{n',n}$ are

$$\hat{H}^{[1]}_{n,l'} = \sum_{\{n',l'\} \in \mathcal{T}_{n,l'}} \omega^{[1]}_{n',n} \check{H}_{n',l'}. \tag{6}$$

The filter coefficients $\omega^{[1]}_{n',n}$ only depend on the frequency index n. This operation is performed in all pilot symbols bearing OFDM symbols. Then the estimate of the second 1D filter is

$$\hat{H}^{[2]}_{n,l} = \sum_{\{n',l'\} \in \mathcal{T}_{n,l'}} \omega^{[2]}_{l',l} \hat{H}^{[1]}_{n,l'}. \tag{7}$$

The filter coefficients $\omega^{[2]}_{l',l}$ depend only on the time index l. The estimates $\hat{H}^{[1]}_{n,l'}$ obtained from the first filtering are used as pilot symbols for the second filtering on subcarrier n. Therefore, the second filtering is done on all N_c subcarriers.

Since in practice, the CF $\theta_{n-n'',l-l''}$ is not perfectly known at the receiver, the filters of the CE have to be designed such

that a great variety of delay power spectral densities (PSDs) and Doppler PSDs are covered. According to [10], a uniform delay PSD ranging from 0 to $\tau_{\max}$ and a uniform Doppler PSD ranging from $-f_{D,\max}$ to $f_{D,\max}$ fulfill these requirements. Then, the discrete frequency CF results in

$$\theta_{n-n''} = \frac{\sin\left(\pi\tau_{\max}(n-n'')F_s\right)}{\pi\tau_{max}(n-n'')F_s} e^{-j\pi\tau_{\max}(n-n'')F_s}, \quad (8)$$

and the discrete time CF yields

$$\theta_{l-l''} = \frac{\sin\left(2\pi f_{D,\max}(l-l'')T_s'\right)}{2\pi f_{D,\max}(l-l'')T_s'}, \quad (9)$$

where T_s' denotes the duration of one OFDM symbol including the guard interval T_g.

2.2. MMSE detection

Equalization according to the MMSE criterion minimizes the mean square value of the error

$$\varepsilon_n = S_n - G_n R_n \quad (10)$$

between the transmitted signal and the output of the equalizer. The MSE $J_n = E\{|\varepsilon_n|^2\}$ can be minimized by applying the orthogonality principle [16], stating that the MSE J_n is minimum if the equalizer coefficient G_n is selected such that the error ε_n is orthogonal to the received signal R_n^*, that is, $E\{\varepsilon_n R_n^*\} = 0$. The equalization coefficients based on the MMSE criterion result in

$$G_n = \frac{H_n^*}{|H_n|^2 + 1/\gamma_c}, \quad (11)$$

where the computation of the MMSE equalization coefficients requires an estimation of the actual SNR per subcarrier γ_c.

2.3. Coded MLSSE

The MLSSE minimizes the symbol error probability, which is equivalent to maximizing the conditional probability $P\{s_\mu^{(k)}|\mathbf{r}\}$ that the data symbol $s_\mu^{(k)}$ of user k was transmitted and the signal $\mathbf{r}$ was received, where $s_\mu^{(k)}$ is one possible transmitted data symbol of user k, $\mu = 1,\ldots,M^K$, and M^K is the number of possible transmitted data symbol vectors. If $K \le L$, the data is a priori known to be 0 for the $L-K$ data symbols. The estimate of $s^{(k)}$ obtained by MLSSE is

$$\hat{s}^{(k)} = \arg\max_{s_\mu^{(k)}} P\{s^{(k)}\,|\,\mathbf{r}\}. \quad (12)$$

The conditional probability $P\{s^{(k)}|\mathbf{r}\}$ is given by

$$P\{s^{(k)}\,|\,\mathbf{r}\} = \sum_{\forall \mathbf{s}_\mu = s^{(k)}} P\{\mathbf{s}_\mu^{(k)}\,|\,\mathbf{r}\}, \quad \mu = 1,\ldots,M^K, \quad (13)$$

where the probability $P\{s^{(k)}|\mathbf{r}\}$ is the union of all mutually exclusive events $P\{\mathbf{s}_\mu^{(k)}|\mathbf{r}\}$ with the same realization of $s^{(k)}$ [16]. By using Bayes' rule and assuming that all data symbols $s^{(k)}$ are equally probable and by noting that $p(\mathbf{r})$ is independent of the transmitted data symbol, the decision rule based on finding the symbol that maximizes $P\{s^{(k)}|\mathbf{r}\}$ is equivalent to finding the symbol that maximizes $p(\mathbf{r}|s^{(k)})$. Thus, with (12) and (13), the most likely transmitted data symbol is

$$\hat{s}_\mu^{(k)} = \arg\max_{s_\mu^{(k)}} \sum_{\forall \mathbf{s}_\mu = s_\mu^{(k)}} \exp\left(-\frac{1}{\sigma^2}\Delta^2\left(\mathbf{s}_\mu^{(k)}, \mathbf{r}\right)\right), \quad (14)$$

where

$$\Delta^2\left(\mathbf{s}_\mu^{(k)}, \mathbf{r}\right) = \left\|\mathbf{r} - \mathbf{H}\mathbf{W}_{\text{rot}}\mathbf{s}_\mu\right\|^2, \quad \mu = 1,\ldots,M^K. \quad (15)$$

The Viterbi decoder uses LLRs of all possible symbols as input, which are calculated by the MLSSE unit. The LLRs for coded MC-CDMA mobile radio systems applying MLSSE are given by using all possible transmitter signals:

$$\mathcal{L}^i = \ln\left(\frac{\sum_{\forall \mathbf{s}_\mu \in D^+} \exp\left(-(1/\sigma^2)\Delta^2(\mathbf{s}_\mu, \mathbf{r})\right)}{\sum_{\forall \mathbf{s}_\mu \in D^-} \exp\left(-(1/\sigma^2)\Delta^2(\mathbf{s}_\mu, \mathbf{r})\right)}\right), \quad (16)$$

where i is the bit index from $0,\ldots,$ bits per symbol $\cdot\,(L-1)$.

2.4. Channel models

The simulations are based on a two-path and a twelve-path time-frequency selective channel model with WSSUS. Table 2 shows the main channel properties of the two channel models. The 12-tap channel model (Channel B) imposes more delay diversity in comparison to the two-tap channel model (Channel A). The guard interval was chosen according to the channel model to ensure that no intersymbol interference and intercarrier interference (ICI) occur. The rate loss due to the guard interval was not taken into account.

3. ROTATED SPREADING

In this section, the possible improvements offered by rotated spreading are explained by using the Hamming distance of the spreading sequence and of the convolutional code.

Each user generates bits, where 0 and 1 are generated with a probability of 0.5 each. The bits of each user are encoded by a convolutional encoder with a minimum Hamming distance d_H. We apply an MC-CDMA system with Q user groups, where each group takes up to K users. Each user has M data symbols which are distributed within one user group to M subgroups. Each subgroup has the size of the spreading block L. The spreading block combines one data symbol of each of the K users, where $L \ge K$. Each spreading block forms L chips with the K data symbols. All L chips form one spreading sequence. Traditionally, Walsh-Hadamard spreading codes are used in the downlink of MC-CDMA systems. They are simple to generate at the transmitter by applying a fast Walsh-Hadamard [17] transformation for each subgroup. At the receiver, the Walsh-Hadamard operation is inverted and the different user data symbols are extracted. In

Table 2: Main channel properties.

Path	Path delay (μs)	Relative average power (dB)	Fading characteristics	Doppler spectrum form
Channel A				
1	0	0	Rayleigh	Jakes
2	60	−3	Rayleigh	Jakes
Channel B				
1	0	0	Rayleigh	Jakes
2	16	−1	Rayleigh	Jakes
3	32	−2	Rayleigh	Jakes
4	48	−3	Rayleigh	Jakes
5	64	−4	Rayleigh	Jakes
6	80	−5	Rayleigh	Jakes
7	96	−6	Rayleigh	Jakes
8	112	−7	Rayleigh	Jakes
9	128	−8	Rayleigh	Jakes
10	144	−9	Rayleigh	Jakes
11	160	−10	Rayleigh	Jakes
12	176	−11	Rayleigh	Jakes

the following, we will derive the different constellations for an exemplarily chosen BPSK system.

The Walsh-Hadamard operation generates up to

$$N_{\mathbf{WH}} = b^L \tag{17}$$

values, where b is two to the power of the number of bits per symbol ($= 2^1$) and L defines the size of the spreading length. $N_{\mathbf{WH}}$ consists of only

$$N_{\text{diff},\mathbf{WH}} = L + 1 \tag{18}$$

different constellations. The major part of all different constellations is 0. The possible chip values are unequally distributed and occur by using the binomial distribution:

$$-L = \binom{L}{0}, -L+2 = \binom{L}{1}, \ldots, 0 = \binom{L}{\frac{L}{2}}, \ldots, L = \binom{L}{L}. \tag{19}$$

The scheme can be applied for QPSK by extending the scheme of BPSK to the second dimension. For QPSK, the Walsh-Hadamard operation generates

$$N_{\mathbf{WH}} = \left(2^2\right)^L \tag{20}$$

values, where only

$$N_{\text{diff},\mathbf{WH}} = (L+1)^2 \tag{21}$$

are different. The QPSK solution can be easily transferred to 4-QAM by rotating all possible chip values by $\pi/4$.

Instead of applying a pure Walsh-Hadamard matrix, we apply rotated spreading factors for each spreading sequence. The advantage is that each of the possible $N_{\text{Rot},\mathbf{WH}}$ constellations is different. Each of the possible constellations can be ascribed out of one of the following:

$$b^L = N_{\text{Rot},\mathbf{WH}} = N_{\mathbf{WH}}. \tag{22}$$

The different constellations allow that all L different positions of the spreading sequences differ. Therefore, the minimum (which equals the maximum) Hamming distance of each spreading sequence is L. The higher minimum Hamming distance improves the performance asymptotically. In comparison, the normal unrotated spreading sequences have only a minimum Hamming distance of 1. This can be easily seen by choosing the same value s for each of the L possible ones. All the L values are multiplied by the Walsh-Hadamard matrix and summed up. The summed sequence is $L \cdot (s, 0, \ldots, 0)$ which means it differs by just one position from the null codeword and therefore has a Hamming distance of 1. In addition, by using $-s$ as a value, the summed sequence would be $L \cdot (-s, 0, \ldots, 0)$. The Hamming distance between all three sequences is 1. The $N_{\text{Rot},\mathbf{WH}}$ different constellations are advantageous in a fading channel. Whenever one out of the L constellations is deeply faded, by using the other constellations, the original signal can be restored more likely. Figure 2 shows the visible difference for a spread BPSK system with and without rotation. Only nine different sequences exist for nonrotated spreading, and for the rotated, there are 256 different ones.

In [7, 9], the authors showed that the minimum Euclidean distance of the L data chips is maximized. The total system is a concatenated system based on an outer and an inner code. The outer code is the convolutional channel code. Each channel code offers a distinct minimum Hamming distance d_H. The Hamming distance defines the ability of the channel code to exploit diversity in a Rayleigh faded channel. Therefore, the slope of the BER performance for channel codes with the same Hamming distance is asymptotically equal for high SNRs. By applying a second inner code, the rotated spreading matrix, the second code provides a second Hamming distance. As it is shown in [17, 18], the overall minimum Hamming distance is the product of both minimum Hamming distances. Therefore, the overall

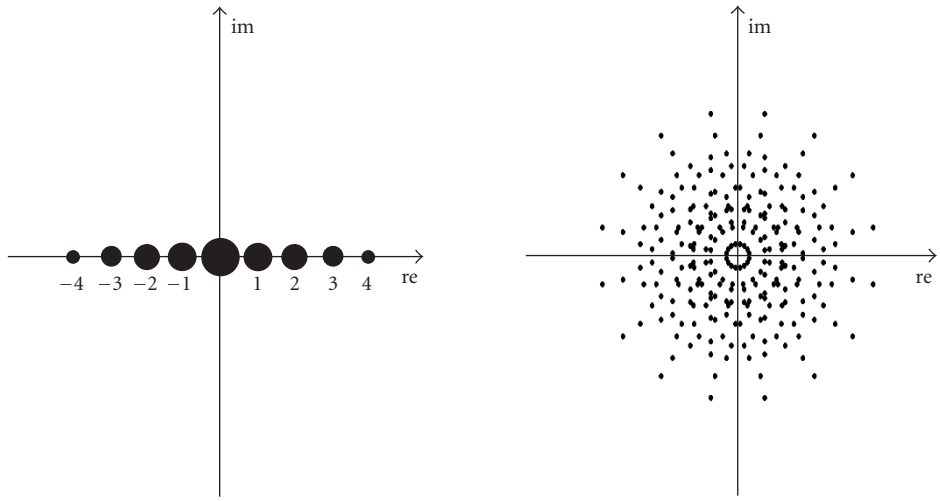

Figure 2: Nonrotated and rotated spreading for BPSK and a spreading length of eight.

performance will asymptotically be better for rotated spreading sequences than the unrotated ones.

4. SIMULATION RESULTS

This section shows the simulation results for rotated versus nonrotated spreading. We investigated uncoded and coded systems with different code rates (and different minimum Hamming distances). In addition, we compared an MMSE and an MLSSE detector and nonperfect channel estimators with perfect channel estimation. Figure 3 depicts the simulation results for the uncoded performance of non- and rotated spreading sequences with channel B. The results for the MMSE show no improvements for rotated case. The MMSE detector is unable to exploit the improved distribution of the Euclidean distance in the signal space. For the MUD, the MLSSE improves the performance significantly. Even further, the single-user bound for a spreading length of eight gains improvement. A longer spreading size allows to distribute the chips over more subcarriers and therefore to exploit more diversity. The gap to the single-user bound is about 1 dB. The performance of an AWGN channel is plotted as a reference. Figure 4 shows performance results for a coded system with robust channel estimation using BPSK as its modulation alphabet. In comparison to Figure 3, the gain for the rotated scenario is noticeable for the MMSE detector and for the MLSSE detector. By applying MLSSE, the gap to the single-user bound is fixed and does not increase for higher SNRs. The loss through the robust channel estimation still does allow the increased minimum Hamming distance to exploit the diversity.

Figure 5 compares the SUD and MUD for channel B. The data is encoded by a convolutional code with rate 3/4 and $d_H = 4$. The lower curve shows the single-user bound for a spreading length of four. The top two curves show the performance of the nonrotated and the rotated spreading matrices using an MMSE detector. The performance is identical

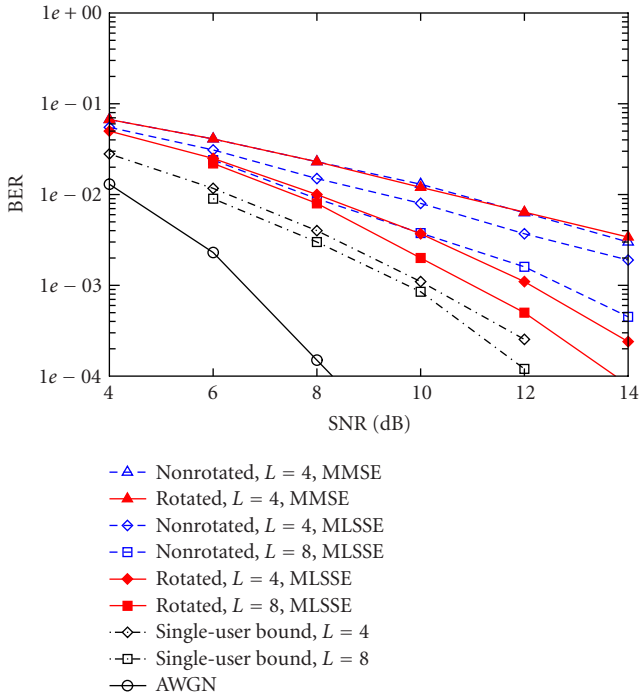

Figure 3: Performance comparison of rotated and nonrotated spreading codes with the MMSE and the MLSSE detectors and variable spreading lengths for an uncoded 4-QAM system. Channel B is applied and the maximum Doppler spread is $f_d = 1\%$.

for both cases and the rotated spreading matrices cannot improve the performance. On the other hand, by applying the MLSSE detector at the receiver, the system improves by about 0.7 dB. Figure 6 compares the robust pilot-aided with the perfect channel estimation for rotated spreading sequences with a code rate of 2/3. The gain for the rotated spreading sequences is nearly 1 dB for a BER of 2×10^{-4}. The robust

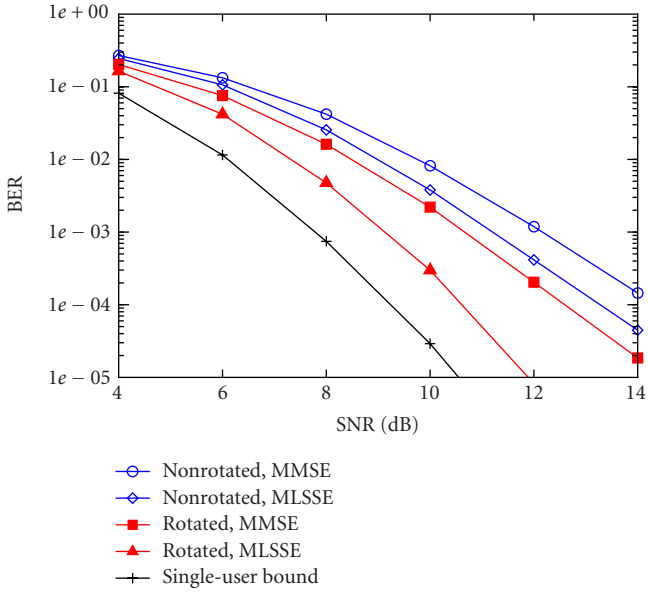

FIGURE 4: Performance comparison of rotated and nonrotated spreading codes with the MMSE and the MLSSE detectors and robust or 2×1-dimensional channel estimation for BPSK. The convolutional code has rate 3/4 and a minimum Hamming distance of $d_{H_{\min}} = 4$.

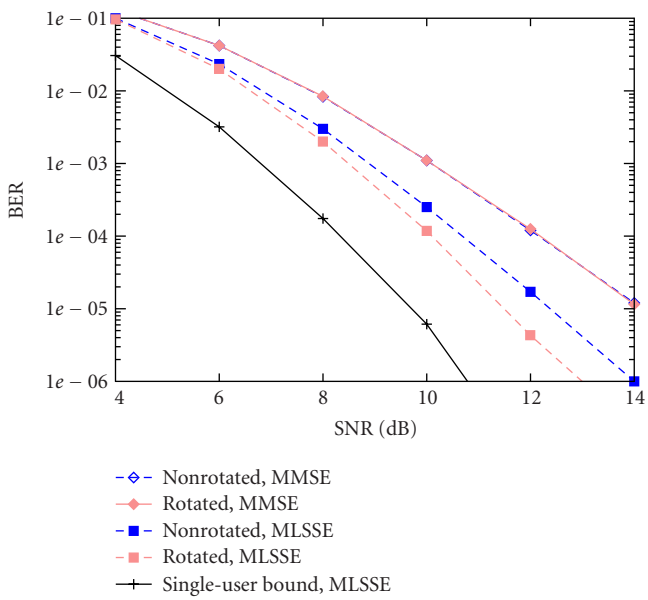

FIGURE 5: Performance comparison of rotated and nonrotated spreading codes with the MMSE and the MLSSE detectors and perfect channel estimation for 4-QAM. The convolutional code has rate 3/4 and a minimum Hamming distance of $d_H = 4$. Note that the MMSE curves for the rotated and the nonrotated are superposed by each other.

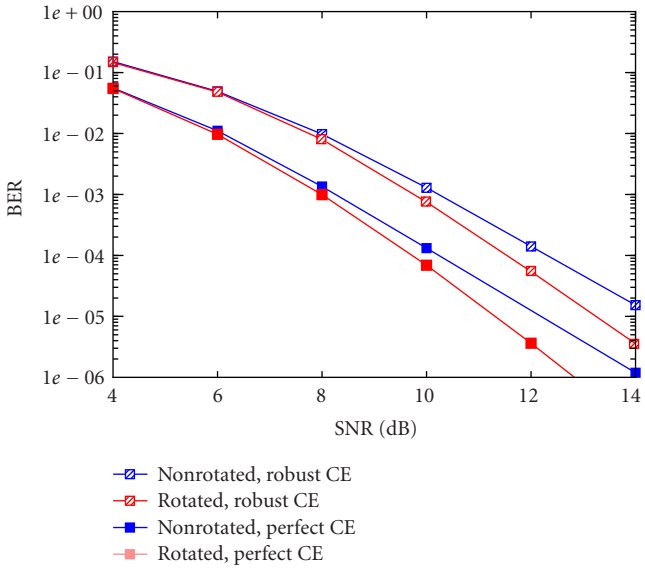

FIGURE 6: Rotated spreading is used for systems applying robust or 2×1-dimensional channel estimation (CE) and perfect channel estimation. Convolutional code is of rate 2/3 and $d_H = 3$. The modulation used is 4-QAM and the MLSSE detector is used.

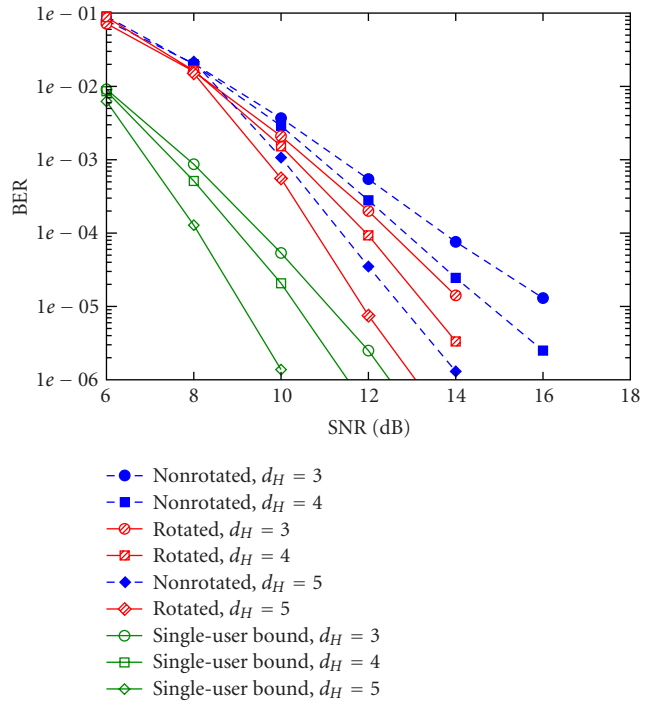

FIGURE 7: Rotated spreading with the MLSSE detector and three different channel codes with $d_H = 3, 4, 5$. The rate is 3/4. Robust channel estimation is performed for 4-QAM modulated data symbols.

channel estimation can maintain the performance gains based on rotated spreading.

In Figure 7, the performance of the rotated and the nonrotated spreading with a convolutional code with rate 3/4 and different minimum Hamming distances d_H of the channel code is shown. The performance gain due to the rotated

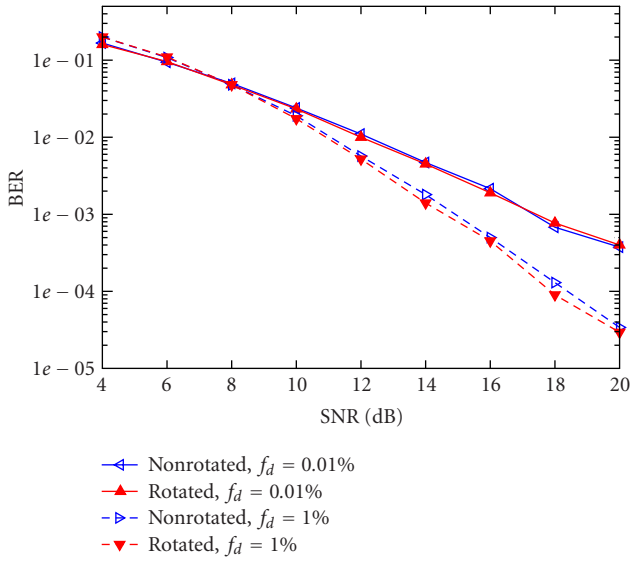

FIGURE 8: For channel A, the performance remains nearly unchanged for systems applying rotated spreading. The maximum Doppler spread is $f_d = 0.01\%$ or $f_d = 1\%$. The convolutional code rate is 3/4 and the minimum Hamming distance is $d_H = 3$. Robust channel estimation for 4-QAM modulated data symbols is used.

spreading is above 1 dB in comparison to the nonrotated spreading. In comparison to Figure 6, the rotated spreading with a $d_{H_{\min}} = 4$ is slightly better than the nonrotated spreading case with $f_d = 1\%$ at a BER of 10^{-4} despite the higher channel coding rate and the higher throughput.

Figure 8 compares the system performance for a 2-tap fading channel (channel A). This channel offers less diversity than channel B. The system performance does slightly differ for the rotated spreading sequences. The additional overall increased minimum Hamming distance for the rotated spreading schemes can not be used to exploit diversity by applying an MLSSE. This improves slightly for high Doppler of 1%.

5. SUMMARY AND OUTLOOK

For BPSK, an MC-CDMA system with rotated spreading matrices improve the performance with SUD and MUD. By applying an MLSSE detector, rotated spreading improves the system performance of a coded and uncoded 4-QAM MC-CDMA system. The performance gain is no longer accessible with an SUD like the MMSE. The performance gain increases as the mobile radio channel offers more diversity than the convolutional channel code could exploit. The rotated spreading allows to exploit the existing diversity even further. The rotated spreading performs, despite a higher throughout with a code rate of 3/4 at a BER of 10^{-4}, better than the unrotated case with a code rate of 2/3. These gains can only be achieved by using an MLSSE detector. The complex detector at the receiver is the major computational burden. For a SUD like the MMSE detector, there is no extra gain noticeable. However, due to the rotation, any loss is not possible, and rotated spreading matrices can be implemented efficiently. The performance improvements depend on the possible complexity of the receiver. A 2×1-dimensional channel estimator was applied to demonstrate that rotated spreading works without loss in comparison to the perfect channel estimator. The overall minimum Hamming distance of the system is increased. The decoding feasibility is not enhanced and therefore for lower SNRs, no improvement can be noted.

The system investigated here is a downlink MC-CDMA system. In the uplink, MC-CDMA is not reasonable due to the high asynchronism between the different users and the uncorrelated transmission channels for the spread sequences. It is more likely that a system like CDM-OFDMA [2] will be applied. The major difference regarding the presented downlink scheme is the combination of the data symbols of one user within one spreading block. Therefore, all chips of one spreading block are effected by the a correlated multipath fading channel. As this scheme is applied in the uplink, the multiuser detector is at the base station and hence the rotated spreading scheme could be an additional source to exploit diversity.

ACKNOWLEDGMENT

The authors would like to thank the anonymous reviewers for their valuable comments.

REFERENCES

[1] S. Verdu, *Multiuser Detection*, Cambridge University Press, Cambridge, UK, 1998.
[2] S. Kaiser, "OFDM code-division multiplexing in fading channels," *IEEE Trans. Communications*, vol. 50, no. 8, pp. 1266–1273, 2002.
[3] K. Boullé and J. C. Belfiore, "Modulation schemes designed for the Rayleigh channel," in *Proc. Conference on Information Sciences and Systems (CISS '92)*, pp. 288–293, Princeton, NJ, USA, March 1992.
[4] K. J. Kerpez, "Constellations for good diversity performance," *IEEE Trans. Communications*, vol. 41, no. 9, pp. 1412–1421, 1993.
[5] V. M. DaSilva and E. S. Sousa, "Fading-resistant modulation using several transmitter antennas," *IEEE Trans. Communications*, vol. 45, no. 10, pp. 1236–1244, 1997.
[6] J. J. Boutros and E. Viterbo, "Signal space diversity: a power- and bandwidth-efficient diversity technique for the Rayleigh fading channel," *IEEE Transactions on Information Theory*, vol. 44, no. 4, pp. 1453–1467, 1998.
[7] C. Lamy and J. J. Boutros, "On random rotations diversity and minimum MSE decoding of lattices," *IEEE Transactions on Information Theory*, vol. 46, no. 4, pp. 1584–1589, 2000.
[8] L. Brunel, "Optimum and sub-optimum multiuser detection based on sphere decoding for multi-carrier code division multiple access systems," in *Proc. IEEE International Conference on Communications (ICC '02)*, vol. 3, pp. 1526–1530, New York, NY, USA, May 2002.
[9] A. Bury, J. Egle, and J. Lindner, "Diversity comparison of spreading transforms for multicarrier spread spectrum transmission," *IEEE Trans. Communications*, vol. 51, no. 5, pp. 774–781, 2003.

[10] K. Fazel and S. Kaiser, *Multi-Carrier and Spread Spectrum Systems*, John Wiley & Sons, Hoboken, NJ, USA, 2003.
[11] J. J. van de Beek and B. M. Popovic, "Benefits of modulation diversity in turbo-coded OFDM systems," in *IEEE Vehicular Technology Conference (VTC '04)*, Milano, Italy, May 2004.
[12] T. Frey and M. Bossert, "A first approach to concatenation of coding and spreading for CDMA-systems," in *Proc. IEEE 4th International Symposium on Spread Spectrum Techniques and Applications (ISSSTA '96)*, vol. 2, pp. 667–671, Mainz, Germany, September 1996.
[13] J. Hagenauer, "Rate-compatible punctured convolutional codes (RCPC codes) and their applications," *IEEE Trans. Communications*, vol. 36, no. 4, pp. 389–400, 1988.
[14] R. Raulefs, A. Dammann, S. Kaiser, and G. Auer, "Rotated spreading sequences for broadband multicarrier-CDMA," in *IEEE 58th Vehicular Technology Conference (VTC '03)*, vol. 2, pp. 862–865, Orlando, Fla, USA, October 2003.
[15] P. Hoeher, S. Kaiser, and P. Robertson, "Pilot-symbol-aided channel estimation in time and frequency," in *Proc. IEEE Global Telecommunications Conference (GLOBECOM '97), Commun. Theory Mini-Conf.*, pp. 90–96, Phoenix, Ariz, USA, November 1997.
[16] A. Papoulis, *Probability, Random Variable and Stochastic Processes*, McGraw-Hill, New York, NY, USA, 1st edition, 1991.
[17] J. G. Proakis, *Digital Communications*, McGraw-Hill, New York, NY, USA, 3rd edition, 1995.
[18] M. Bossert, *Kanalcodierung*, B. G. Teubner, Stuttgart, Germany, 1998.

Ronald Raulefs studied electrical engineering at the University of Kaiserslautern, Germany. From November 1997 till June 1998, he joined the University of Edinburgh, Scotland, as an Erasmus Student. In 1999, he received the Dipl.-Ing. degree from the University of Kaiserslautern, Germany. Since 1999, he has been working as a Researcher at the Institute of Communications and Navigation, the German Aerospace Center (DLR), Oberpfaffenhofen, Germany. His main interests are adaptive antennas and detection techniques in multicarrier systems.

Armin Dammann studied electrical engineering from 1991 to 1997 at the University of Ulm, Germany, with main topic information- and microwave-technology. In July 1997, he received the Dipl.-Ing. degree from the University of Ulm. Since 1997, Armin Dammann is a research staff member at the Institute of Communications and Navigation, the German Aerospace Center (DLR). He has been involved in several research projects with a focus on navigation signal design for Galileo (ESA-SDS), MAC layer design and simulations for a future aeronautical VHF digital link (fVDL), physical layer design and simulations for a "multimedia car platform" (MCP), and design and simulation for a 4th generation mobile air interface based on MC-CDMA.

Stephan Sand received the M.S. degree in electrical engineering from the University of Massachusetts Dartmouth, USA, and the Dipl.-Ing. degree in communications technology from the University of Ulm, Germany, in 2001 and 2002, respectively. He is currently working toward the Ph.D. degree at the Institute of Communications and Navigation, German Aerospace Center (DLR), Oberpfaffenhofen, Germany. From January to April 2004, he was a Visiting Researcher at the NTT DoCoMo R&D Center, Yokosuka, Japan, working in the area of MC-CDMA and channel estimation. His main research interests include various aspects of mobile communications and signal processing, such as time-frequency methods for signal processing, space-time signal processing, MC-CDMA, channel estimation, and multiuser detection.

Stefan Kaiser received the Dipl.-Ing. and Ph.D. degrees in electrical engineering from the University of Kaiserslautern, Germany, in 1993 and 1998, respectively. Since 1993, he has been with the Institute of Communications and Navigation, German Aerospace Center (DLR), Oberpfaffenhofen, Germany, where he is currently the Head of the Mobile Radio Transmission Group. In 1998, he was a Visiting Researcher at the Telecommunications Research Laboratories (TRLabs) in Edmonton, Canada, working in the area of wireless communications. His current research interests include multicarrier communications, multiple access schemes, and space-time processing for mobile radio applications. Dr. Kaiser is the Coorganizer of the International Workshop Series on Multi-Carrier Spread Spectrum (MC-SS), and he is the Coauthor of the book "*Multi-Carrier and Spread Spectrum Systems*" (John Wiley & Sons, 2003) and Coeditor of the book series "*Multi-Carrier Spread Spectrum & Related Topics*" (Kluwer Academic Publishers, 2000–2004). He is also the Guest Editor of several special issues on multicarrier spread spectrum of the European Transactions on Telecommunications (ETT). He is the Cochair of the IEEE ICC 2004 Communication Theory Symposium. He is a Senior Member of the IEEE and Member of the VDE/ITG.

Gunther Auer received the Dipl.-Ing. degree in electrical engineering from the University of Ulm, Germany, in 1996, and the Ph.D. degree from the University of Edinburgh, UK, in 2000. From 2000 to 2001, he was a Research and Teaching Assistant with the University of Karlsruhe (TH), Germany. Since 2001, he has been a Senior Research Engineer at NTT DoCoMo Euro-Labs, Munich, Germany. His research interests include multicarrier-based communication systems, multiple access schemes, and statistical signal processing, with an emphasis on channel estimation and synchronization techniques.